

# Super Water- and Oil-Repellent Surfaces on Intrinsically Hydrophilic and Oleophilic Porous Silicon Films

Liangliang Cao, Tyler P. Price, Michael Weiss, and Di Gao\*

Department of Chemical and Petroleum Engineering, University of Pittsburgh,  
Pittsburgh, Pennsylvania 15261

Received October 31, 2007. In Final Form: December 31, 2007

We demonstrate that porous Si films fabricated by a convenient gold-assisted electroless etching process, which possess a hierarchical porous structure consisting of micrometer-sized asperities superimposed onto a network of nanometer-sized pores, are able to induce a superhydrophobic phenomenon on an intrinsically hydrophilic hydrogen-terminated Si surface and a superoleophobic phenomenon on an intrinsically oleophilic self-assembled monolayer-coated Si surface. Through comparison with porous Si films consisting of vertically aligned straight pores, which are hydrophilic and oleophilic, we show that an overhang structure resulting from the hierarchical porous structure is essential to preventing water and oil from penetrating the texture of the films and inducing the observed macroscopic superhydrophobic and superoleophobic phenomena.

## I. Introduction

Surfaces with water contact angles of greater than 150° are typically referred to as superhydrophobic or super water-repellent. Such surfaces are often observed in nature on plant leaves<sup>1,2</sup> and insect legs<sup>3</sup> and wings.<sup>4,5</sup> Water on these surfaces beads up and drips off rapidly while washing away powderlike contamination. This phenomenon renders materials with superhydrophobic surfaces self-cleaning. The observed self-cleaning property of natural superhydrophobic surfaces has stimulated extensive research interest in the fabrication of artificial superhydrophobic surfaces as well as in understanding the fundamental mechanisms underlying the behavior of a liquid on such surfaces.<sup>6–13</sup> However, one challenge to the self-cleaning property of superhydrophobic surfaces is oil contamination—these surfaces repel water but not oil. Therefore, surfaces that are both super water-repellent and super oil-repellent (with oil contact angles of greater than 150°) have received considerable attention for their potential applications in green construction, water- and oil-repellent materials, self-cleaning products, and microfluidic systems.<sup>1–10,14,15</sup>

The wettability of a solid surface is determined by two factors, namely, its chemical nature and its topographic structure. Modifying the surface with chemical groups that have a low surface free energy can effectively increase the water and oil contact angles of a solid surface. To date, the trifluoromethyl group (CF<sub>3</sub>)-terminated surface has been reported to possess the

lowest surface free energy and correspondingly the highest water (about 120°) and oil contact angles on a flat surface.<sup>16,17</sup> To increase the contact angles, the surfaces need to be roughened. Typically, if the contact angle of a flat surface ( $\theta_{\text{flat}}$ , also referred to as the intrinsic contact angle of the surface) is greater than 90°, then roughening the surface will result in an apparent contact angle ( $\theta_{\text{rough}}$ ) that is greater than  $\theta_{\text{flat}}$ ; if  $\theta_{\text{flat}}$  is less than 90°, then roughening will result in a  $\theta_{\text{rough}}$  that is less than  $\theta_{\text{flat}}$ . Therefore, artificial superhydrophobic surfaces have been made by either creating a rough topography on a hydrophobic material or modifying a rough surface by chemical compositions with a low surface free energy.<sup>10–13</sup> Either approach requires a  $\theta_{\text{flat}}$  of greater than 90° in order to increase the hydrophobicity by tuning the surface topography.

The  $\theta_{\text{flat}}$  of a liquid on a solid surface can be correlated to the surface free energy of the solid ( $\gamma_s$ ), the liquid ( $\gamma_l$ ), and the interface between the solid and the liquid ( $\gamma_{sl}$ ) by Young's equation

$$\cos \theta_{\text{flat}} = \frac{\gamma_s - \gamma_{sl}}{\gamma_l} \quad (1)$$

where  $\gamma_{sl}$  can be estimated by<sup>18</sup>

$$\gamma_{sl} = \gamma_s + \gamma_l - 2\sqrt{\gamma_s\gamma_l} \quad (2)$$

Following these correlations, to achieve a  $\theta_{\text{flat}}$  of greater than 90°, a  $\gamma_s$  of less than ~20 mN/m is needed for water (with a  $\gamma_l$  of ~72 mN/m), and a  $\gamma_s$  of less than ~6 mN/m is needed for most alkanes with a  $\gamma_l$  of 20–30 mN/m. If a  $\theta_{\text{flat}}$  of greater than 90° is indeed needed to increase the contact angle by roughening the surface, then very few materials can be used to make super oil-repellent surfaces. For example, Teflon is known to possess a low  $\gamma_s$  (~18.5 mN/m) among most commonly used materials, but it still does not satisfy the requirement ( $\gamma_s$  needs to be less than ~6 mN/m) to make it super oil-repellent. (CF<sub>3</sub>)-terminated surfaces (with a  $\gamma_s$  of ~6 mN/m), in principle, can barely satisfy

\* Corresponding author. E-mail: gaod@engr.pitt.edu. Tel: (412) 624-8488. Fax: (412) 624-9639.

- (1) Neinhuis, C.; Barthlott, W. *Ann. Bot. (London)* **1997**, *79*, 667–677.
- (2) Barthlott, W.; Neinhuis, C. *Planta* **1997**, *202*, 1–8.
- (3) Gao, X. F.; Jiang, L. *Nature* **2004**, *432*, 36–36.
- (4) Barbieri, L.; Wagner, E.; Hoffmann, P. *Langmuir* **2007**, *23*, 1723–1734.
- (5) Lee, W.; Jin, M. K.; Yoo, W. C.; Lee, J. K. *Langmuir* **2004**, *20*, 7665–7669.
- (6) Quere, D. *Rep. Prog. Phys.* **2005**, *68*, 2495–2532.
- (7) Lafuma, A.; Quere, D. *Nat. Mater.* **2003**, *2*, 457–460.
- (8) Herminghaus, S. *Europhys. Lett.* **2000**, *52*, 165–170.
- (9) Marmur, A. *Langmuir* **2004**, *20*, 3517–3519.
- (10) Coffinier, Y.; Janel, S.; Addad, A.; Blossey, R.; Gengembre, L.; Payen, E.; Boukherroub, R. *Langmuir* **2007**, *23*, 1608–1611.
- (11) Erbil, H. Y.; Demirel, A. L.; Avci, Y.; Mert, O. *Science* **2003**, *299*, 1377–1380.
- (12) Feng, L.; Li, S. H.; Li, Y. S.; Li, H. J.; Zhang, L. J.; Zhai, J.; Song, Y. L.; Liu, B. Q.; Jiang, L.; Zhu, D. B. *Adv. Mater.* **2002**, *14*, 1857–1860.
- (13) Suzuki, S.; Nakajima, A.; Yoshida, N.; Sakai, M.; Hashimoto, A.; Kameshima, Y.; Okada, K. *Langmuir* **2007**, *23*, 8674–8677.
- (14) Wenzel, R. N. *Ind. Eng. Chem.* **1936**, *28*, 988.
- (15) Cassie, A. B. D.; Baxter, S. *Trans. Faraday Soc.* **1944**, *40*, 546.

(16) Tsujii, K.; Yamamoto, T.; Onda, T.; Shibuichi, S. *Angew. Chem., Int. Ed. Engl.* **1997**, *36*, 1011–1012.

(17) Shibuichi, S.; Yamamoto, T.; Onda, T.; Tsujii, K. *J. Colloid Interface Sci.* **1998**, *208*, 287–294.

(18) Israelachvili, J. N. *Intermolecular and Surface Forces*, 2nd ed.; Academic Press: New York, 1991; pp 144–145.

this requirement. However, to experimentally obtain  $(\text{CF}_3)$ -terminated surfaces with such a low  $\gamma_s$  has been proven to be challenging. Therefore, although super oil-repellent surfaces have been reported, the oil contact angles in the literature are often reported using oils with a relatively high  $\gamma_1$  ( $> 30$  mN/m) such as polyols, esters, arenes, and/or their mixtures.<sup>16,17</sup> As a matter of fact, surfaces that possess a contact angle of greater than  $150^\circ$  for alkanes (such as hexadecane) with  $\gamma_1$  between 20 and 30 mN/m have rarely been reported.

Recent investigations have demonstrated that it is possible to induce superhydrophobic phenomena on intrinsically hydrophilic materials if the surface consists of microtextures with overhang structures.<sup>19,20</sup> The overhang structures are able to prevent water from penetrating the texture as a result of the capillary force. As a result, water is in contact with a composite surface of air and solid. Such a state has been referred to as the Cassie state, which induces the observed macroscopic superhydrophobic behavior. A question of significant interest is whether this principle can be applied to make super oil-repellent surfaces on intrinsically oleophilic materials because it will greatly expand the range of materials that can be used to manufacture the super oil-repellent surfaces. Most recently, Tuteja et al. have fabricated superoleophobic surfaces with “re-entrant surface curvatures” following this principle.<sup>21</sup>

In this letter, we demonstrate a convenient approach to the fabrication of porous silicon (Si) films that are able to induce a superoleophobic phenomenon on intrinsically oleophilic surfaces. The porous Si films are fabricated by a gold-assisted electroless etching process, which produces a hierarchical porous structure that consists of micrometer-sized asperities superimposed onto a network of tilted nanometer-sized pores. The hierarchical porous structure forms textures with overhang structures on the surface, which are able to induce a superhydrophobic phenomenon on the intrinsically hydrophilic Si surface. After being coated with fluorinated organic molecules, the porous Si films are super oil-repellent to diethylene glycol and hexadecane with a  $\theta_{\text{rough}}$  of greater than  $150^\circ$ , although the coated Si surface is intrinsically oleophilic with a  $\theta_{\text{flat}}$  of less than  $90^\circ$  for these oils. It is speculated that this superoleophobic phenomenon is induced by the overhang structures present on the surface following the same mechanism that induces the superhydrophobic phenomenon on intrinsically hydrophilic materials.

## II. Experimental Section

**Preparation of Porous Si Films.** Two types of porous Si films were prepared in our experiment—one has tilted pores and the other has vertically aligned straight pores. The first type of porous Si was prepared by a gold (Au)-assisted electrochemical etching process. P-type (111) Si wafers (boron-doped,  $1\text{--}10\ \Omega\ \text{cm}$ ) purchased from Silicon Quest International, Inc. were used. They were diced to  $1\ \text{cm} \times 1\ \text{cm}$  chips for the experiment. The Si surface was first coated with Au nanoclusters, which served as the electrochemical reaction center during the etching step. The Au coating solution was made by dissolving  $0.01\ \text{M}\ \text{KAuCl}_4$  (99.995%, Aldrich) in a 10 wt % HF aqueous solution (EMD). The Si chips were dipped in the coating solution at room temperature for 30 s. The Si chips were then etched in an etching solution at  $50\ ^\circ\text{C}$  for a variety of periods. The etching solution was made by dissolving  $0.135\ \text{M}\ \text{Fe}(\text{NO}_3)_3$  (Fisher Scientific) in a 10 wt % HF aqueous solution. After the etching process, the samples were rinsed with ethanol and deionized (DI) water sequentially and finally dried with nitrogen gas.

The second type of porous Si with vertically aligned straight pores was prepared by the anodic etching of (100) silicon chips. The p-type (100) silicon wafers (boron-doped,  $<1\ \text{m}\Omega\ \text{cm}$ ) were purchased from Siltronic (France) and then diced into  $2\ \text{cm} \times 2\ \text{cm}$  chips. A Teflon electrochemical cell that exposed  $1.6\ \text{cm}^2$  of the Si chip was employed for the anodic etching process. The etching solution consisted of a 3:1 (v/v) 48% aqueous HF/ethanol solution. A direct current at a density of  $100\ \text{mA}/\text{cm}^2$  was applied for 10 min. After the etching process, the samples were rinsed with ethanol and DI water sequentially and finally dried with nitrogen gas.

**Self-Assembled Monolayer (SAM) Coating.** Prior to the coating process, the samples were exposed to ultraviolet ozone (UVO) (Jelight Inc.) for 15 min at room temperature to oxidize the Si surface. The samples were then immersed in the SAM coating solution, made by dissolving  $0.5\ \text{mM}$  (tridecafluoro-1,1,2,2,-tetrahydrooctyl) trichlorosilane (FTS) ( $n\text{-C}_{13}\text{F}_{27}\text{CH}_2\text{CH}_2\text{SiCl}_3$ , Gelest Inc.) into a 4:1 (v/v) mixture of hexadecane (anhydrous, Sigma-Aldrich)/chloroform (anhydrous, Sigma-Aldrich). After about 15 min of coating in the SAM solution, the samples were thoroughly rinsed with isooctane (Sigma-Aldrich), isopropanol (Fisher Scientific), and DI water, sequentially.

**Characterization.** Scanning electron microscopy (SEM) images were taken by a Philips XL-30 field-emission SEM setup. The contact angle was measured using a VCA-OPTIMA drop shape analysis system (AST Products, Inc.) with a computer-controlled liquid dispensing system and a motorized tilting stage. Droplets of liquids in a volume of  $5\ \mu\text{L}$  were used to measure the static contact angle. The advancing and receding angles were recorded during the expansion and contraction of the droplets induced by placing a needle in the water droplets and continuously supplying and withdrawing water through the needle. The sliding angle was measured by tilting the stage and recorded when the droplet began to move in the downhill direction. The experiments were performed under normal laboratory ambient conditions ( $20\ ^\circ\text{C}$  and 40% relative humidity). Each contact angle measurement was repeated three times at different places on the sample, and the mean value was reported.

## III. Results and Discussion

Au-assisted electroless etching processes have been previously employed to prepare silicon nanowires.<sup>22</sup> The process is applied here to make hierarchical porous structures on Si. Au clusters were first deposited onto the Si surface via a galvanic displacement reaction mechanism by dipping the Si chip in an aqueous solution containing  $\text{KAuCl}_4$  and HF.<sup>23</sup> The chip was then transferred to an etching solution containing  $\text{Fe}(\text{NO}_3)_3$  and HF, where pores were formed by oxidizing Si while reducing  $\text{Fe}^{3+}$ . The Au clusters coated onto the Si prior to the etching step are believed to serve as the local electrodes that attract electrons from the silicon underneath and facilitate silicon oxidation and dissolution during the etching process.<sup>22</sup> Therefore, pores are formed where the Au clusters are present, and the Au clusters sink into the pores as the etching proceeds. Because the etching prefers to proceed along the Si  $\langle 100 \rangle$  direction on a Si (111) surface, tilted pores are formed. Figure 1a,b shows the representative top and cross-sectional SEM images of the as-fabricated porous silicon films after 1 h of etching. A network of tilted pores on the nanometer scale is clearly seen in these images. In addition, asperities in the micrometer scale are observed, and the topography of the asperities is superimposed onto the network of nanometer pores.

The as-fabricated sample was superhydrophobic. The static water contact angle was measured to be  $\sim 160^\circ$  (Figure 1b inset). The hysteresis—the difference between the advancing and receding angles—was measured to be less than  $2^\circ$ , and water

(19) Cao, L. L.; Hu, H. H.; Gao, D. *Langmuir* **2007**, *23*, 4310–4314.

(20) Cao, A.; Cao, L.; Gao, D. *Appl. Phys. Lett.* **2007**, *91*, 034102.

(21) Tuteja, A.; Choi, W.; Ma, M.; Mabry, J. M.; Mazzella, S. A.; Rutledge, G. C.; McKinley, G. H.; Cohen, R. E. *Science* **2007**, *318*, 1618–1622.

(22) Peng, K. Q.; Hu, J. J.; Yan, Y. J.; Wu, Y.; Fang, H.; Xu, Y.; Lee, S. T.; Zhu, J. *Adv. Funct. Mater.* **2006**, *16*, 387–394.

(23) Gao, D.; He, R. R.; Carraro, C.; Howe, R. T.; Yang, P. D.; Maboudian, R. *J. Am. Chem. Soc.* **2005**, *127*, 4574–4575.

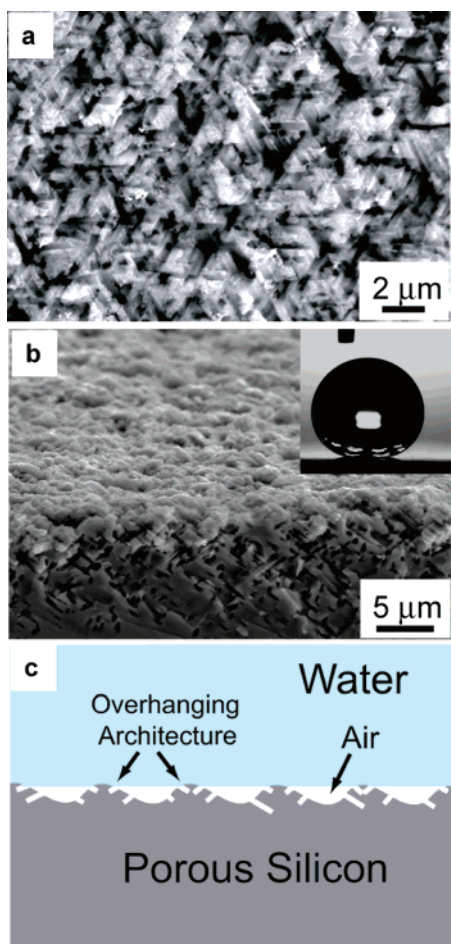


**Figure 1.** Porous silicon surface fabricated by Au-assisted electroless etching. (a) Top-view SEM image. (b) Cross-sectional-view SEM image. The inset is an optical image of a water droplet on the surface. (c) Schematic cross-sectional profile of water in contact with the porous silicon surface.

droplets ( $\sim 5 \mu\text{L}$ ) roll off of the substrate at a sliding angle of less than  $2^\circ$ . Because no organic chemicals are involved in the entire fabrication process and the intrinsic water contact angle of hydrogen-terminated Si is less than  $90^\circ$ , we attribute the observed superhydrophobic phenomenon to the hierarchical topographic characteristic of the porous Si.

As schematically shown in Figure 1c, the superimposition of the micrometer-scale asperities onto the network of nanometer pores forms overhang structures, which may induce the observed superhydrophobic phenomenon on the intrinsically hydrophilic silicon surface.<sup>8,19–21</sup> Figure 2 schematically shows two cross-sectional profiles of liquid in contact with the as-fabricated porous silicon. Two critical parameters in these profiles are (i) the angle ( $\theta_{\text{overhang}}$ ) formed between the side walls of the indent and the horizontal line and (ii) the intrinsic contact angle ( $\theta_{\text{flat}}$ ) of the substrate. When  $\theta_{\text{overhang}}$  is greater than  $\theta_{\text{flat}}$  (Figure 2a), the liquid–air interface (or meniscus) inside the indent produces a capillary force that draws the liquid into the pores. As a result, the liquid is in complete contact with silicon, a state that has been referred to as a Wenzel state. When  $\theta_{\text{overhang}}$  is less than  $\theta_{\text{flat}}$  (Figure 2b), the liquid–air interface inside the indent produces a capillary force that is able to prevent liquid from entering the indent. Therefore, the liquid is in contact with a composite surface of solid and air, a state that has been referred to as a Cassie state.

When water is in contact with the freshly prepared porous Si with a hydrogen-terminated Si surface,  $\theta_{\text{flat}}$  is about  $80^\circ$ , which is greater than  $\theta_{\text{overhang}}$  as observed from the SEM image (Figure

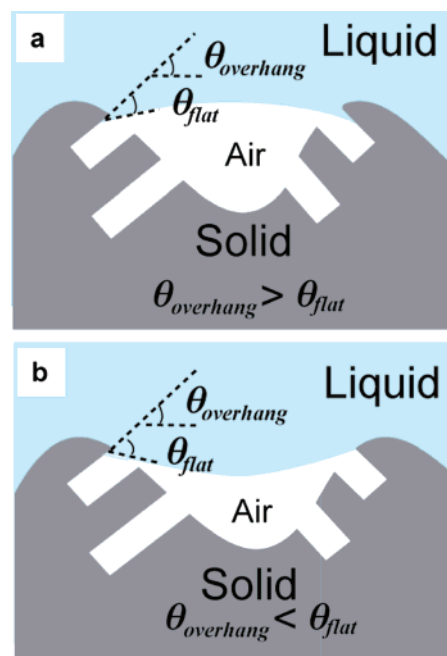


**Figure 2.** Schematic cross-sectional profile of liquid in contact with the porous silicon surface consisting of overhang structures in the case of (a)  $\theta_{\text{overhang}} > \theta_{\text{flat}}$  and (b)  $\theta_{\text{overhang}} < \theta_{\text{flat}}$ .

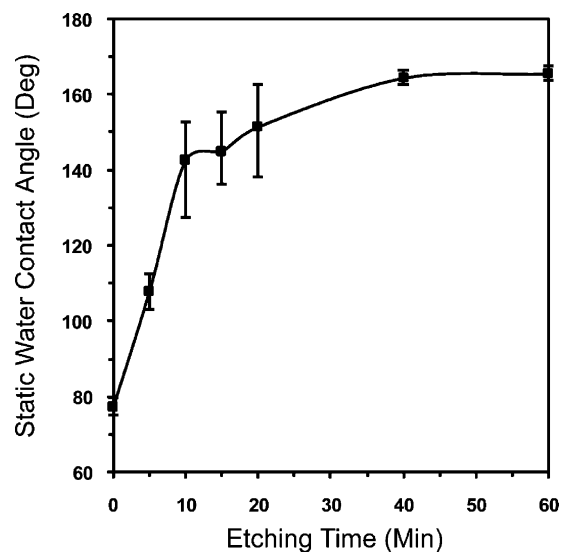


**Figure 3.** Static water contact angle measured on the porous Si with tilted pores as a function of the etching time.

1). Therefore, the profile of water in contact with porous Si is represented in Figure 2b. In the Cassie state, the correlation between the apparent contact angle ( $\theta_{\text{rough}}$ ) and the intrinsic contact angle ( $\theta_{\text{flat}}$ ) has been described by the Cassie–Baxter equation<sup>15</sup>

$$\cos \theta_{\text{rough}} = \phi_s \cos \theta_{\text{flat}} - (1 - \phi_s) \quad (3)$$

where  $\phi_s$  is the area fraction of the solid surface in contact with liquid. On the freshly prepared porous Si with a hydrogen-terminated Si surface corresponding to a  $\theta_{\text{rough}}$  of  $\sim 160^\circ$ ,  $\phi_s$  is approximately 0.05. The experiment was repeated on porous Si samples prepared by varying the etching time, which produced surfaces with varied  $\phi_s$ . The static water contact angles (WCAs) on these samples were measured and plotted in Figure 3. It was observed that the static WCA increased from  $\sim 102$  to  $162^\circ$  as the etching time increased from 5 to 40 min, whereas after 40 min, etching the Si for a longer time did not significantly increase



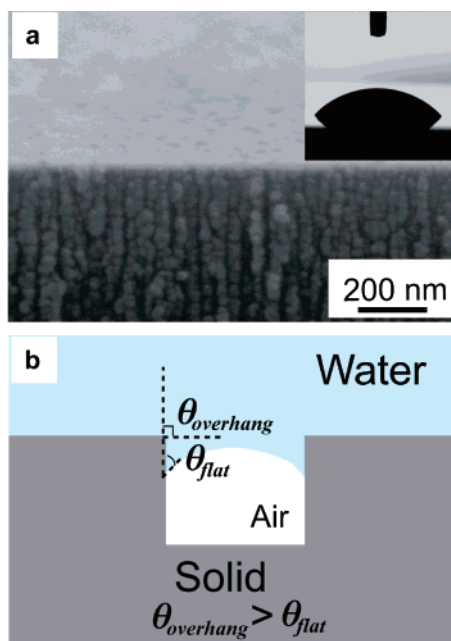


**Figure 4.** Water in contact with the porous Si with vertically aligned straight pores. (a) Representative SEM image of the porous silicon with vertically aligned straight pores. The inset is an optical image of a water droplet on the surface. (b) Schematic cross-sectional profile of water in contact with the porous silicon surface, where  $\theta_{\text{overhang}} > \theta_{\text{flat}}$ .

the contact angle. The increase in the WCA as a function of the etching time is likely due to a decrease in  $\phi_s$  when the Si is etched for a longer time.

To prove the important role that the surface topography plays in inducing the superhydrophobic phenomenon on the Si surface with tilted pores, porous Si with vertically aligned straight pores was fabricated by anodic etching, and the wetting phenomenon on such porous Si surfaces was examined. Figure 4a shows an SEM image of the as-fabricated porous silicon by anodic etching. The nanometer-sized pores are vertically aligned along the surface normal direction of the Si chip, and no micrometer-sized asperities are present on the surface. The porous Si surfaces with straight pores are hydrophilic. When water is in contact with such surfaces (schematically shown in Figure 4b), without the presence of overhang structures, the capillary force will draw water into the pores. As a result, water is in complete contact with silicon. In the Wenzel state,  $\theta_{\text{rough}}$  can be correlated to  $\theta_{\text{flat}}$  by the following equation<sup>14</sup>

$$\cos \theta_{\text{rough}} = r \cos \theta_{\text{flat}} \quad (4)$$

where  $r$  is the roughness factor defined as the ratio of the actual surface area to its projection area on a flat surface. If  $\theta_{\text{flat}}$  is less than  $90^\circ$ , then  $\theta_{\text{rough}}$  is less than  $\theta_{\text{flat}}$ . In our experiment,  $\theta_{\text{rough}}$  on the porous Si with straight pores is measured to be  $\sim 40^\circ$ , which is significantly lower than  $\theta_{\text{flat}}$  of about  $80^\circ$ .

Intrigued by the superhydrophobic phenomenon observed on intrinsically hydrophilic porous Si films, we further investigated the wetting properties of oil on the porous Si surfaces with tilted pores both before and after coating them with organic molecules. Porous Si samples prepared by 1 h of etching (Figure 1) were used in these experiments. The wetting properties were evaluated using two oils: diethylene glycol and hexadecane with surface

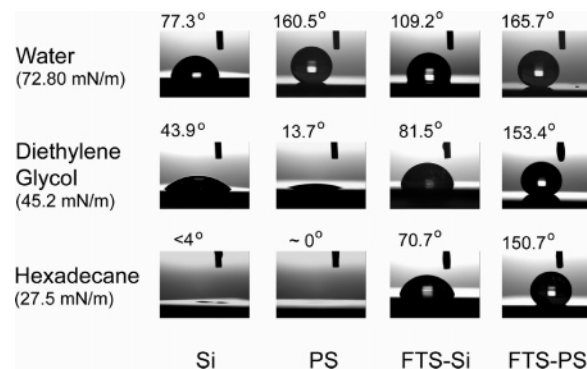


**Figure 5.** Static contact angles of water, diethylene glycol, and hexadecane on flat silicon (Si), porous silicon (PS) with tilted pores, flat silicon coated with FTS (FTS-Si), and porous silicon with tilted pores coated with FTS (FTS-PS).

tensions of 45.2 and 27.5 mN/m, respectively. Before coating the sample with organic molecules, the porous Si surfaces are oleophilic (Figure 4). The contact angles of diethylene glycol and hexadecane were both measured to be less than  $15^\circ$ . This result is expected because  $\theta_{\text{flat}}$  of diethylene glycol and hexadecane are about  $40$  and  $3^\circ$ , respectively, on hydrogen-terminated Si surfaces; these values are smaller than  $\theta_{\text{overhang}}$  of the porous Si film. In the case shown in Figure 2a, these oils are in complete contact with Si.

After coating the flat Si with a self-assembled monolayer of FTS, the  $\theta_{\text{flat}}$  values of water, diethylene glycol, and hexadecane on the FTS-coated Si were measured to be  $109.2$ ,  $81.5$ , and  $70.7^\circ$ , respectively. When the coating was applied to porous Si films, the coated films were super oil-repellent with  $\theta_{\text{rough}}$  of greater than  $150^\circ$  for both diethylene glycol and hexadecane (Figure 5). This is interesting considering the fact that the FTS-coated Si is intrinsically oleophilic with  $\theta_{\text{flat}}$  of less than  $90^\circ$  for both oils. We speculate that such super oil-repellency is induced by the same mechanism that induces the superhydrophobic phenomenon on intrinsically hydrophilic porous Si films. Because  $\theta_{\text{flat}}$  of oil is larger than  $\theta_{\text{overhang}}$  after coating the surface with FTS, the overhang structures can prevent oil from penetrating the texture (Figure 2b). Therefore, the oil is in contact with a composite surface of air and solid (the Cassie state) and exhibits an apparent contact angle of greater than  $150^\circ$ .

In conclusion, we have demonstrated a convenient approach to the fabrication of porous Si films that are able to induce a superhydrophobic phenomenon on an intrinsically hydrophilic Si surface and a superoleophobic phenomenon on an intrinsically oleophilic FTS-coated Si surface. The hierarchical porous structure of the films forms overhang structures on the surface, and these play an important role in inducing the superhydrophobic and superoleophobic phenomena. Certainly, problems such as the dynamic behavior of the oils on the superoleophobic surfaces and the quantitative evaluation of the stability of the Cassie state still need further investigation. Nonetheless, it is anticipated that the demonstrated approach and principle could be applied to expand the range of materials that can be used to fabricate superhydrophobic and, in particular, superoleophobic surfaces.

**Acknowledgment.** This work was supported by the National Science Foundation (grant no. CMMI 0626045) and the University of Pittsburgh Mascaro Sustainability Initiative.

LA703401F